ANNALS OF MULTIDISCIPLINARY RESEARCH, INNOVATION AND TECHNOLOGY (AMRIT)

(A peer-reviewed open access multidisciplinary journal)

www.adtu.in/amrit

RESEARCH ARTICLE

NANOTECHNOLOGY

# Synthesis and Characterization of $SnO_2$ Nanoparticles for the Development of Ultraviolet Photodetectors

Minakshee Sarma[1], Nairika Deka[1], Sunandan Baruah[1*]

[1]Centre of Excellence in Nanotechnology, Assam down town University, Panikhaiti, Guwahati, Assam-781026, India
[*]Corresponding author: Sunandan Baruah, *Email: sunandan.baruah@adtu.in*

Article Chronicle: Received: 22/05/24 Accepted: 26/06/24 Published: 30/06/24

**Abstract**

Tin dioxide nanoparticles ($SnO_2$ Nanoparticles) are wide-bandgap semiconductor material that can be used in various applications in photodetector in Ultraviolet (UV) range below 400 nm wave length. In the present work, $SnO_2$ NPs were used as UV sensing material integrated in a sensor setup. The $SnO_2$ NPs were imaged through Transmission Electron Microscopy from which the diameter of the spherical nanoparticles was measured to be 50nm. The optical bandgap was calculated from UV-visible spectrograph to be 4.48 eV using Tauc plot. The response of the $SnO_2$ NPs based photodetector was observed after illumination using a UV light (10 lumen on the sensor). The transition time of the photodetector was found to be 1 sec and maximum current recorded was 0.1 mA.

**Keywords:** *Nanoparticles, $SnO_2$, Photodetector, Bandgap, UV*

## 1 Introduction

Photodetectors (PDs) are the most important optoelectronic devices that have sparked a lot of research because of their exact ability to convert light into electrical impulses(1). It has great potential in applications of imaging, telecommunication, and biological sensing due to which the expansion of the photoelectronic sector has increased during the last few decades. Due to some significant characteristics of semiconducting materials which have large band gaps can be used for UV photoconductivity. Many processes, such as light absorption, carrier photogeneration, and carrier movement, are involved in photoconductivity(2). It is commonly recognized that a typical photodetector needs to have the following characteristics of "5S": fast speed, high stability, high spectral selectivity, high signal-to-noise ratio, and high sensitivity(3; 4). UV-A (wavelengths between 400 and 320 nm), UV-B (wavelengths between 320 and 280 nm), UV-C (wavelengths between 280 and 200 nm), and far UV (wavelengths between 200 and 10 nm, which reaches the X-ray spectral low energy frontier) are the four spectral regions that are commonly used to categorize UV light(5). The ozone layer in the atmosphere absorbs most of the UV radiation from the Sun. Wavelengths longer than 280 nm in the sun's spectrum can pass through the atmosphere and reach Earth. For this reason, "solar-blind" UV detectors are those that exhibit great sensitivity to UV-C and far UV radiation in comparison to radiation with wavelengths longer than 280 nm. UV detectors that are more sensitive to UV-A, UV-B, UV-C, and far UV radiation than to radiation with wavelengths longer than 400 nm are said to as "visible-blind" since visible light spans the wavelength range from 400 to 700 nm(4; 5). Wide band gap semiconductors are extensively used in ultraviolet (UV) detectors(1). From vacuum diodes, photomultipliers(6), and silicon photodiodes to the third generation of wide band gap semiconductor-based UV detectors, the study of UV detectors has evolved significantly. Nanostructured metal oxide viz. ZnO, $SnO_2$, $TiO_2$, $Cu_2O$, $Ga_2O_3$, $Fe_2O_3$, $In_2O_3$, CdO, $CeO_2$ etc. (7; 8) semiconductors have been presented as a solution for UV detectors with weak signal detection, high quantum efficiency, low power consumption, and improved responsiveness due to their distinct physical and chemical features(9). As one-dimensional nanostructures are low dimensional and therefore subject to quantum confinement phenomena, they display intriguing electrical and optical features(10). Due to this various structural and morphological forms of tin ox-

ide ($SnO_2$) 1D nanomaterials have been fabricated over the past several years, including nanowires(11; 12), nanoribbons or nanobelts, and nanorods(13). Also with a wide band gap of 3.6–3.8 eV, $SnO_2$ is a direct band gap semiconductor that exhibits transparency in the visible spectrum and a significant exciton binding potential of 130 meV (14). Additionally, it could be a useful material for UV photodetectors. Due to their optical and electrical characteristics, $SnO_2$ nanoparticles can be used to develop UV photodetectors(15). However, research indicates that the low performance of devices made of pure nanostructured $SnO_2$ in UV detection is caused by surface imperfections and the trapping effect of oxygen molecules adsorbed on the $SnO_2$ NP's surface(16). As a result, a lot of work has gone into raising the efficiency of $SnO_2$-based photodetectors. In this work, hydrothermally synthesized $SnO_2$ NPs was used to design, fabricate and test a UV photodetector. The NPs were characterized by using TEM and UV Vis spectroscopy and the Tauc plot was used to estimate the optical bandgap of the NPs.

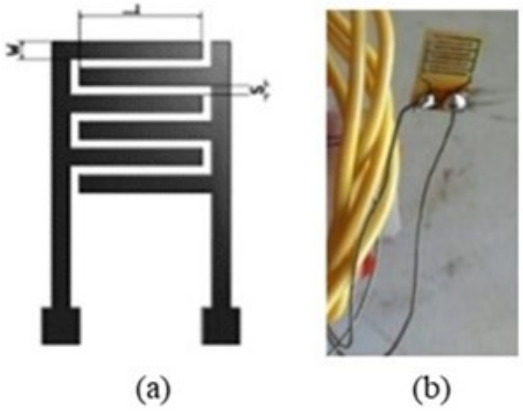


Figure 1: (A) Electrode Design in Diptrace Software (B) Fabricated $SnO_2$ Based Photodetector

## 2 Experimental Work

### 2.1 Materials

Tin chloride ($SnCl_4 \cdot 5\,H_2O$), Cetyltrimethylammonium bromide ($C_{16}H_{33})\,N\,((CH_3)_3Br$, CTAB), Ferric chloride ($FeCl_3$) and ammonia solution ($NH_4OH$) were purchased from Otto Chemica, Himedia, SRL and Emparta, respectively. De-ionised water was collected from Centre of Excellence in Nanotechnology (CoEN) at Assam down town University. Diptrace software was used for designing the electrode pattern with a gap of 0.4mm. Printed circuit boards were procured from local electronic stores for the fabrication of the sensors.

### 2.2 Design of Electrodes

The gap in the interdigitated electrode was maintained 0.4 mm. The design of the electrode was imported to a PCB followed by an etching process. Figure 1 shows the design of electrode using Diptrace Software. The designed electrode was kept in $FeCl_3$ solution for 1 hour for etching. It was then thoroughly washed with DI water so that only the copper pattern was left.

### 2.3 Synthesis of SnO2 NPs

2mM $SnCl_4 \cdot 5\,H_2O$ and 2mM CTAB was added in 50 ml DI water under vigorous stirring. Then the pH of the solution was maintained near 8 by adding ammonia dropwise. The prepared solution was then transferred to an autoclave and kept at 110°C for 24 hours.

### 2.4 Fabrication of Photodetector

A thin layer of $SnO_2$ nanoparticles was deposited on the designed electrode using a dip and dry method. Then it was annealed for 1 hour at 90°C, and the two free ends of the electrode were connected with wires to form the $SnO_2$ based photodetector.

### 2.5 Characterization

UV-Vis spectroscopy was used to examine the optical characteristics of the synthesized $SnO_2$ nanoparticles. For this an Ocean Insight UV-visible spectrophotometer. Beer Lambert's law which is represented in Equation 1 has been used to measure absorbance.

$$Absorbance = \log\left(\frac{I_0}{I}\right) = \varepsilon cL \quad (1)$$

where "c" stands for concentration, "L" for the length of the light path inside the medium, and stands for the molar absorptivity. "I0" and "I" represent the intensities of the light absorbed by the sample and the reference, respectively. For the UV-Vis analysis, the spectrophotometer spanned a wavelength range of 200 to 1000 nm.

## 3 Results and Discussion

The synthesized $SnO_2$ nanoparticles are spherical with diameters approximately 8 nm as was calculated from measurements carried out on 50 nanoparticles in a TEM micrograph shown in Figure 2. As the NPs are semiconducting in nature, their TEM images are not prominent as some electrons pass through the samples. Some of the NPs are therefore circled for visibility. The particle size distribution is shown in Figure 2 which shows dominance of particles in the range of 8-10 nm.

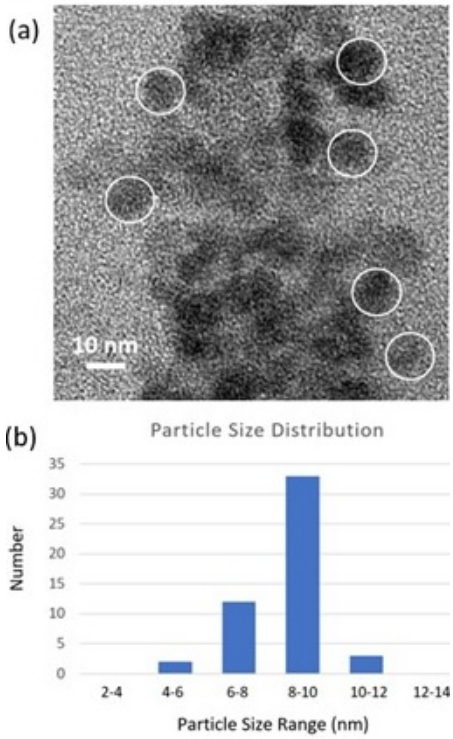


Figure 2: TEM Micrograph of the $SnO_2$ NPs (B) Particle Size Distribution Showing Dominance in the Range 8-10 Nm

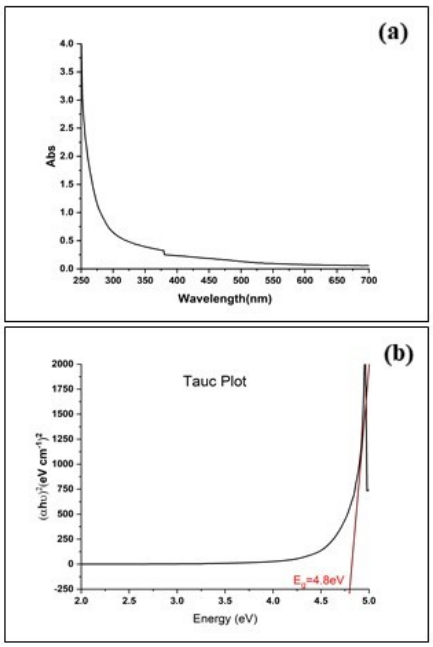


Figure 3: (A) UV Vis Spectra of SnO2 NPs in DI Water (B) Tauc Plot with Band Gap 4.8 EV of SnO2 NPs

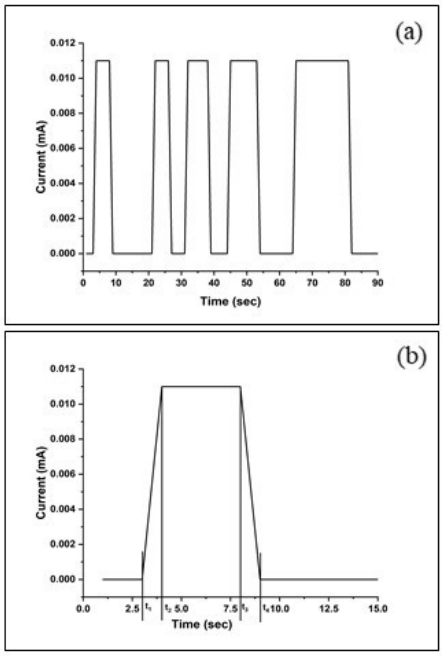


Figure 4: (A) Current Vs Time Response of $SnO_2$ Nps Based Photodetector (B) Response and Decay Times of the Sensor Output to UV Illumination

The Figure 3 shows the UV Vis absorbance spectrum of $SnO_2$ NPs. An absorbance peak near 390 nm confirms the formation of $SnO_2$ Nps. Figure 3 shows the Tauc Plot of $SnO_2$ NPs generated from the plot in Figure 3, where the optical band gap was calculated to be 4.8 eV. The optical bandgap of bulk $SnO_2$ is 3.6 eV and the increase in the bandgap can be attributed to the small size of the nanoparticles.

The Figure 4 shows the current vs time characteristics of the $SnO_2$ Nps based photodetector. The conductivity of the sensor was observed when the UV LED was turned ON and OFF; the current rises to a peak point when turned ON and drops when it was OFF. The transition time was observed to be 1 sec from the graph and the maximum current in the presence of UV light was .01mA. This demonstrates that the developed $SnO_2$ Nps based photodetector exhibits the highest current when exposed to UV light. The $SnO_2$ NPs based photodetector does not exhibit any conductivity when exposed to other visible or infra-red light. When the illumination was triggered at t1, the sensor reached a stable state at t2. Similarly, when the light was switched off at t3, the sensor output reached the ground state at t4. The response time tr= t2-t1 was calculated to be 1.00 sec and the decay time td = t4-t3 was calculated to be 1.04 sec which are comparable (tr td).

## 4 Conclusion

$SnO_2$ Nps are extensively utilized in photodetector applications due to their large bandgap. We have synthesized $SnO_2$ Nps using a solvothermal method. The confirmation of nanoparticle formation was achieved through the use of TEM and UV Vis spectroscopy. A photodetector was

fabricated by depositing the synthesized $SnO_2$ Nps on cu electrodes etched out on PCBs. The photodetector's reaction was examined by a time-current graph, which demonstrated conductivity only under ultraviolet (UV) light. The reaction time was observed to be 1 sec which could be repeated with precision.

## Conflict of Interest

The authors declare no conflict of interest in this reported communication.

## Acknowledgment

The authors acknowledge the Centre of Excellence in Nanotechnology (CoEN) at Assam down town University for the experimental facilities.

## References

[1] Z. Li, K. Xu, and F. Wei, "Recent progress in photodetectors based on low-dimensional nanomaterials," *Nanotechnology Reviews*, vol. 7, no. 5, pp. 393–411, 2018.

[2] R. Borgohain and S. Baruah, "Design and analysis of uv detector using zno nanorods on interdigitated electrodes," *ADBU Journal of Engineering Technology*, vol. 4, 2016.

[3] Z. Huang, J. Zhu, Y. Hu, Y. Zhu, G. Zhu, L. Hu, Y. Zi, and W. Huang, "Tin oxide (sno2) nanoparticles: facile fabrication, characterization, and application in uv photodetectors," *Nanomaterials*, vol. 12, no. 4, p. 632, 2022.

[4] L. Sang, M. Liao, and M. Sumiya, "A comprehensive review of semiconductor ultraviolet photodetectors: from thin film to one-dimensional nanostructures," *Sensors*, vol. 13, no. 8, pp. 10 482–10 518, 2013.

[5] U. Soni, V. Shukla, R. C. Prajapati, and S. Surve, "Structural, electrical and optical studies of zno/tio2thin films fabricated by rf sputtering process for uv application."

[6] F. Cao, Y. Liu, M. Liu, Z. Han, X. Xu, Q. Fan, and B. Sun, "Wide bandgap semiconductors for ultraviolet photodetectors: Approaches, applications, and prospects," *Research*, 2024.

[7] M. S. Chavali and M. P. Nikolova, "Metal oxide nanoparticles and their applications in nanotechnology," *SN applied sciences*, vol. 1, no. 6, p. 607, 2019.

[8] T. Zhai, X. Fang, M. Liao, X. Xu, H. Zeng, B. Yoshio, and D. Golberg, "A comprehensive review of one-dimensional metal-oxide nanostructure photodetectors," *Sensors*, vol. 9, no. 8, pp. 6504–6529, 2009.

[9] Y. Zou, Y. Zhang, Y. Hu, and H. Gu, "Ultraviolet detectors based on wide bandgap semiconductor nanowire: A review," *Sensors*, vol. 18, no. 7, p. 2072, 2018.

[10] S. Baruah and J. Dutta, "Hydrothermal growth of zno nanostructures," *Science and technology of advanced materials*, vol. 10, no. 1, p. 013001, 2009.

[11] H. W. Kim and S. H. Shim, "Synthesis and properties of sno2 one-dimensional nanomaterials on pt-coated substrates," in *Materials science forum*, vol. 517. Trans Tech Publ, 2006, pp. 21–24.

[12] Z. R. Dai, Z. W. Pan, and Z. L. Wang, "Novel nanostructures of functional oxides synthesized by thermal evaporation," *Advanced Functional Materials*, vol. 13, no. 1, pp. 9–24, 2003.

[13] S. Mathur, S. Barth, H. Shen, J.-C. Pyun, and U. Werner, "Size-dependent photoconductance in sno2 nanowires," *Small*, vol. 1, no. 7, pp. 713–717, 2005.

[14] X. Pan, T. Zhang, Q. Lu, W. Wang, and Z. Ye, "High responsivity ultraviolet detector based on novel sno 2 nanoarrays," *RSC advances*, vol. 9, no. 64, pp. 37 201–37 206, 2019.

[15] P. Sharma and S. Sawyer, "S7-n5: Sno 2 colloidal nanoparticles based ultraviolet photodetector with high signal to noise ratio," in *2014 Lester Eastman Conference on High Performance Devices (LEC)*. IEEE, 2014, pp. 1–4.

[16] L. Gan, M. Liao, H. Li, Y. Ma, and T. Zhai, "Geometry-induced high performance ultraviolet photodetectors in kinked sno 2 nanowires," *Journal of Materials Chemistry C*, vol. 3, no. 32, pp. 8300–8306, 2015.